

Millisecond Pulsars in Dense Star Clusters: Evolution, Scaling Relations, and the Galactic-Center Gamma-ray Excess

CLAIRE S. YE^{1,2,3} AND GIACOMO FRAGIONE^{1,2}

¹*Department of Physics & Astronomy, Northwestern University, Evanston, IL 60208, USA*

²*Center for Interdisciplinary Exploration & Research in Astrophysics (CIERA), Northwestern University, Evanston, IL 60208, USA*

³*Canadian Institute for Theoretical Astrophysics, University of Toronto, 60 St. George Street, Toronto, Ontario M5S 3H8, Canada*

ABSTRACT

The number of millisecond pulsars (MSPs) observed in Milky Way globular clusters has increased explosively in recent years, but the underlying population is still uncertain due to observational biases. We use state-of-the-art N -body simulations to study the evolution of MSP populations in dense star clusters. These cluster models span a wide range in initial conditions, including different initial masses, metallicities, and virial radii, which nearly cover the full range of properties exhibited by the population of globular clusters in the Milky Way. We demonstrate how different initial cluster properties affect the number of MSPs, for which we provide scaling relations as a function of cluster age and mass. As an application, we use our formulae to estimate the number of MSPs delivered to the Galactic Center from inspiralling globular clusters to probe the origin of the Galactic-Center gamma-ray excess detected by *Fermi*. We predict about 400 MSPs in the Galactic Center from disrupted globular clusters, which can potentially explain most of the observed gamma-ray excess.

1. INTRODUCTION

Since the discovery of a highly-magnetized, fast-spinning, radio-pulsating neutron star (NS) around 50 years ago (Hewish et al. 1968), our understanding of these stellar remnants has grown tremendously. They can now be observed across the electromagnetic spectrum, from the radio to X-rays and gamma-rays, and even in gravitational waves (e.g., Kaspi 2010; Abbott et al. 2017). NSs are ubiquitous in the Universe, and have close connections to a number of current puzzles in astronomy, including the origins of the mysterious Fast Radio Bursts (e.g., Petroff et al. 2022, and references therein).

NSs in the form of millisecond pulsars (MSPs) and X-ray binaries are especially abundant in globular clusters¹, where the MSP specific abundance is about an order of magnitude larger than the one in the Galactic field (Clark 1975; Katz 1975; Ransom 2008). It is now well understood that the frequent gravitational encounters dictated by the high stellar densities of globular clusters efficiently catalyze the dynamical formation

of MSPs (e.g., Bhattacharya & van den Heuvel 1991; Sigurdsson & Phinney 1995; Ivanova et al. 2008; Ye et al. 2019). These past few years have seen a rapid increase in the number of detected cluster MSPs thanks to the advent of new radio telescopes, such as *FAST* and *MeerKAT* (e.g., Pan et al. 2021; Ridolfi et al. 2021). However, the true underlying pulsar population is still rather uncertain owing to selection biases, including the luminosity thresholds of surveys, the dispersion by the interstellar medium, the spreading of pulsar signals by Doppler shifting in binaries, and the beaming fraction (e.g., Lorimer 2008, for a review).

Many previous studies have estimated the pulsar population in star clusters using different methods, including pulsar luminosity functions (Fruchter & Goss 1990; Kulkarni et al. 1990; Wijers & van Paradijs 1991; Hui et al. 2010; Bagchi et al. 2011), binary population synthesis with a cluster background (Ivanova et al. 2008), combining stellar encounter rates with observations (X-ray sources, Heinke et al. 2005; gamma-ray luminosities, Abdo et al. 2010), and Bayesian analysis (e.g., Turk & Lorimer 2013). However, different methods have yielded very different results and no studies have explored systematically the population of cluster pulsars with self-consistent globular cluster simulations.

In the past decade, MSPs from globular clusters have been connected to the Galactic-Center gamma-ray ex-

Corresponding author: Claire S. Ye
shiye2015@u.northwestern.edu

¹ <http://www.naic.edu/~pfreire/GCpsr.html>

cess detected by the *Fermi*-Large Area Telescope (Goodenough & Hooper 2009). This gamma-ray excess is roughly spherical symmetric about the Galactic Center, and extends out to ~ 2 kpc, which cannot be explained by the cosmic ray interaction with interstellar medium or other known gamma-ray sources (e.g., Murgia 2020). The two main competing explanations for the excess are dark matter annihilation and/or an unresolved MSP population (e.g., Hooper & Goodenough 2011; Hooper & Linden 2011; Abazajian 2011; Abazajian & Kaplinghat 2012; Murgia 2020, and references therein). While the former scenario is challenged by the non-detection of gamma-rays from dwarf spheroidal galaxies (Murgia 2020), the small number of low-mass X-ray binaries, which are believed to be the progenitors of MSPs (e.g., Alpar et al. 1982; Bhattacharya & van den Heuvel 1991), detected in the Galactic Center (Cholis et al. 2015; Haggard et al. 2017) argues against the in-situ MSP hypothesis (although see Gautam et al. 2022). Instead, previous studies have suggested that MSPs delivered by globular clusters that inspiraled into the Galactic central region may explain the excess (Brandt & Kocsis 2015; Abbate et al. 2018; Fragione et al. 2018).

In this study, we systematically explore a large number of cluster models simulated with the *N*-body Monte Carlo code `Cluster Monte Carlo` (CMC; Kremer et al. 2020) to calculate the number of MSPs in globular clusters with a wide range in initial conditions, including different initial masses, metallicities, and virial radii. We derive scaling relations as a function of the cluster mass and age, which we then apply to estimate the population of MSPs delivered to the Galactic Center by inspiraling globular clusters. Compared to previous studies that estimated the number of MSPs (e.g., Fruchter & Goss 1990; Kulkarni et al. 1990; Wijers & van Paradijs 1991; Heinke et al. 2005; Ivanova et al. 2008; Abdo et al. 2010; Hui et al. 2010; Bagchi et al. 2011; Turk & Lorimer 2013) or their gamma-ray luminosities in dense star clusters (e.g., Brandt & Kocsis 2015; Abbate et al. 2018; Fragione et al. 2018; Naiman et al. 2020), our approach is more realistic since the catalog models include a self-consistent detailed treatment of single and binary pulsar evolution in a dynamical environment, and are representative of the Milky Way globular clusters.

Our paper is organized as follows. In Section 2, we discuss how the number of MSPs in globular clusters depends on the clusters' properties, and provide scaling relations to estimate their number as a function of cluster mass and age. In Section 3, we estimate the population of MSPs delivered to the Galactic Center from inspiralling globular clusters and compare their gamma-ray luminosity to the observed Galactic-Center gamma-

ray excess. We discuss the implications of our finding and draw our conclusions in Section 4.

2. MILLISECOND PULSAR POPULATION IN GLOBULAR CLUSTERS

2.1. *N*-body Models

We use the CMC cluster catalog models (Kremer et al. 2020) to estimate the population of MSPs in globular clusters. These catalog models were run with the CMC *N*-body dynamics code (e.g., Rodriguez et al. 2021, and references therein), which is based on the Hénon-style orbit-averaged Monte Carlo method (Hénon 1971a,b). The models span a wide range of initial conditions, including different initial numbers of stars ($N = 2 \times 10^5$, 4×10^5 , 8×10^5 , 1.6×10^6), Galactocentric distances ($R_g/\text{kpc} = 2, 8, 20$), virial radii ($R_v/\text{pc} = 0.5, 1, 2, 4$), and metallicities ($Z = 0.0002, 0.002, 0.02$). The initial stellar density distributions in the models follow a King profile (King 1966) with a concentration parameter $W_0 = 5$. The initial masses of the stars are drawn from a Kroupa initial mass function (IMF; Kroupa 2001) between 0.08 and $150 M_\odot$. All models have a 5% initial binary fraction where the masses of the companion stars are drawn from a flat distribution in mass ratio to the primary star in the range $[0.1 - 1]$ (e.g., Duquennoy & Mayor 1991). The initial binary separations are sampled from a log-uniform distribution from near contact ($a \geq 5(R_1 + R_2)$, where R_1 and R_2 are the stellar radii) to the hard/soft boundary, and the initial binary eccentricities follow a thermal distribution (e.g., Heggie 1975). Finally, the natal kicks of NSs formed in core-collapse supernovae are sampled from a Maxwellian distribution with a standard deviation $\sigma_{ccsn} = 265 \text{ km s}^{-1}$ (Hobbs et al. 2005), while NSs formed in electron-capture supernovae and accretion-induced collapses receive smaller natal kicks drawn from a Maxwellian distribution with a standard deviation $\sigma_{eccsn} = 20 \text{ km s}^{-1}$ (Kiel et al. 2008; Ye et al. 2019). All models are evolved up to a Hubble time, and they reproduce well the observed properties of the population of Galactic globular clusters (Kremer et al. 2020, and their Figure 2).

In our cluster models, MSPs are modeled following Ye et al. (2019, and references therein). In short, NSs are all assumed to be born as young pulsars with large magnetic fields between $10^{11.5} - 10^{13.8}$ G and spin periods between 30 ms and 1000 ms. MSPs are formed during periods of stable mass transfer from their companion stars in binaries. As a result of Roche lobe overflow, the young pulsar or the old non-radiating NS will be spun up by the mass and angular momentum transferred from the inner edge of a Keplerian accretion disc (Hurley et al. 2002, Eq. 54), and its magnetic field will decay following

$$B = \frac{B_0}{1 + \frac{\Delta M}{10^{-6} M_\odot}} \exp\left(-\frac{T - t_{\text{acc}}}{\tau}\right) + 5 \times 10^7 \text{ G}, \quad (1)$$

where B_0 is the magnetic field at the beginning of the mass transfer period, t_{acc} is the time spent on accretion, and $\tau = 3$ Gyr is the decay timescale of the magnetic field of isolated pulsars. We assume a lower limit of 5×10^7 G for the MSP magnetic fields. Note that our simple prescriptions allow us to reproduce closely the observed magnetic fields and spin periods of cluster pulsars, as shown in Ye et al. (2019).

2.2. Gamma-ray luminosity and Millisecond Pulsar Population

The *Fermi* Gamma-ray Space Telescope has detected gamma-ray emission from a number of globular clusters, generally thought to originate from MSPs therein present. To compare our models against observations, we estimate the total gamma-ray luminosity of our cluster models from their population of MSPs. The gamma-ray luminosities of model MSPs are calculated using (see Hooper & Mohlabeng 2016, Eq. 3.3)

$$L_{\gamma \text{MSP}} \approx 4.8 \times 10^{33} \left(\frac{B}{10^{8.5} \text{ G}}\right)^2 \left(\frac{P}{3 \text{ ms}}\right)^{-4} \left(\frac{\eta}{0.1}\right) \text{ erg/s}, \quad (2)$$

where B and P are the magnetic field and spin period of a MSP, respectively, and η , which we fix to 0.1, is the gamma-ray luminosity emission efficiency. Figure 1 shows the observed gamma-ray luminosities per unit mass from 25 globular clusters detected by *Fermi* (Hooper & Linden 2016, Table 1), and model gamma-ray luminosities from 70 catalog models with a non-zero number of MSPs (within the last 2 Gyr). We find that most of our models well overlap with the region defined by the observed population². As already discussed, our models are consistent with the observed Galactic globular cluster properties such as their masses and half-light radii. Figure 1 illustrates that our catalog models can also reproduce the observed gamma-ray luminosities of Galactic globular clusters quite well.

² The outliers where $L_\gamma/M \lesssim 10^{28} \text{ erg s}^{-1} M_\odot^{-1}$ are from ~ 10 models with different initial conditions. All of them except one has only one MSP (one model has four MSPs) within the last 2 Gyrs. Most of these MSPs have low gamma-ray luminosities because they were formed early in the evolution of their host clusters and evolved in isolation where their magnetic fields decayed to $\lesssim 10^8$ G and they spun down slightly, or they went through more mass transfer periods and their magnetic fields were further reduced. Therefore, the offsets from the observations are from a small number of MSPs combined with their low gamma-ray luminosities.

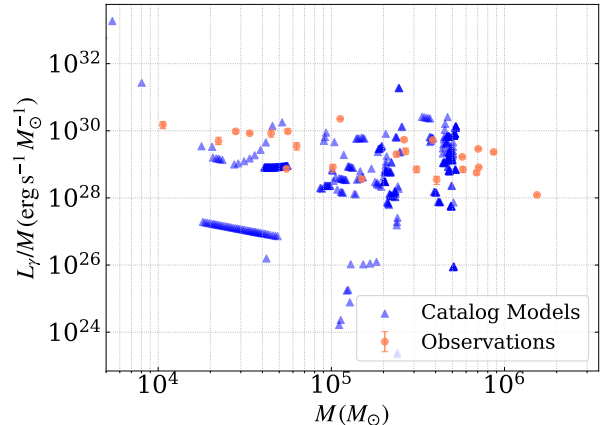


Figure 1. Gamma-ray luminosity per cluster mass as a function of the cluster mass. We show gamma-ray luminosities from multiple time steps, within 2 Gyrs until either the time of cluster disruption or a Hubble time. We only show model clusters that survived to the present day or dissolved after 7 Gyr, which is about the age of the known youngest globular clusters in the Milky Way (Forbes & Bridges 2010; Dotter et al. 2010, 2011; VandenBerg et al. 2013; Kruijssen et al. 2019, and references therein)

To further break down the MSP number dependence on the properties of a globular cluster, we show in Figure 2 the numbers of MSPs for models with metallicity $Z = 0.002$, Galactocentric distance $R_g = 8$ kpc, and various initial numbers of stars N and viral radii R_v . Models with different metallicities and Galactocentric distances are shown in Figure 8-15 in the Appendix. We find that the most massive and densest globular clusters with initial $N \geq 8 \times 10^5$ and $R_v = 0.5$ pc contribute the largest number of MSPs (see Figures 2 and 8-15). This is expected since the more massive and denser a globular cluster is, the higher is its dynamical interaction rate, which is the key process to form MSPs (Bhattacharya & van den Heuvel 1991; Sigurdsson & Phinney 1995; Ivanova et al. 2008; Ye et al. 2019).

2.3. Scaling Relations

We calculate the average number of MSPs for catalog models that survived to the present day (see Table 6 in Kremer et al. 2020, for surviving globular clusters), and express the averages as a function of the cluster age with a polynomial function. The polynomial parameters can be taken to be linear functions of the initial numbers of cluster stars or the initial cluster masses M , where $N = M/0.6M_\odot$ for a canonical Kroupa IMF. Our polynomial fits comparing to the model data are shown in Figure 3.

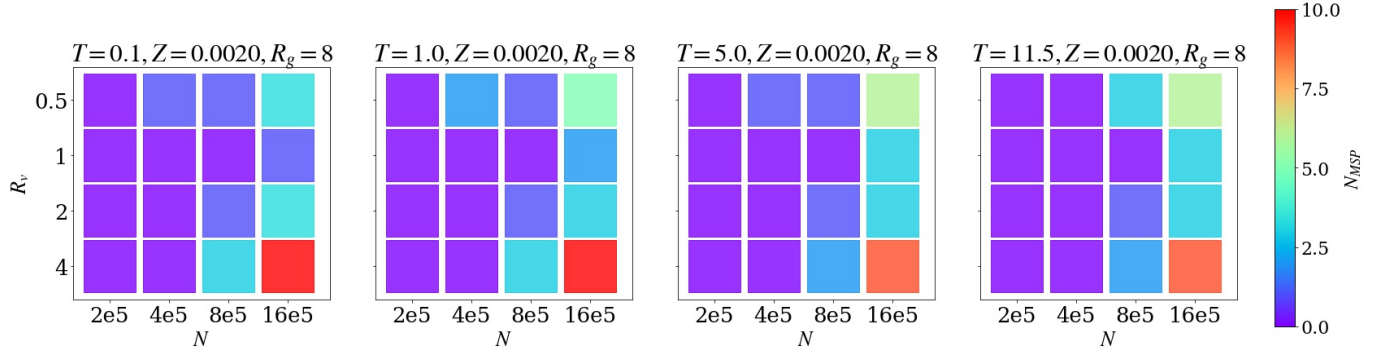


Figure 2. Numbers of MSPs for models with different initial numbers of stars N and virial radii R_v . All models have metallicity $Z = 0.002$ and Galactocentric distance $R_g = 8$ kpc. From left to right the panels show the numbers of MSPs at 0.1, 1., 5., and 11.5 Gyr, respectively.

The polynomial fits as a function of the cluster age and the initial cluster mass are as follows

$$\begin{aligned}
 N_{MSP} &= A \times t + B \times t^2 + C \times t^3 + D \times t^4 + E, \\
 A &= 0.046 \times M_5 - 0.060, \\
 B &= -0.011 \times M_5 + 0.008, \\
 C &= 0.0011 \times M_5 - 0.0003, \\
 D &= -0.00003 \times M_5 - 0.00001, \\
 E &= 0.089 \times M_5 - 0.104,
 \end{aligned} \tag{3}$$

where $M_5 = M/(0.6 \times 10^5 M_\odot)$ and t is in unit of Gyr. Note that the number of MSPs for different N (or M) could have large fluctuations (see Figures 2 and 8-15) because of the different initial conditions and small number statistics. The standard deviations can be up to a factor of about 2 the average values for dense star cluster models with $N > 2 \times 10^5$.

The initial cluster mass can be estimated from the present-day mass taking into account the fact that most catalog models that survived to the present day lost $\sim 50 - 60\%$ of their initial mass depending on their galactocentric distance (in our models the mean value is about 60% and the median is about 55%; the mass loss rate for models with $R_g = 2$ kpc is about 10% larger for both values)³. As an example, we estimate the number of MSPs in the globular cluster 47 Tucanae, assuming its present-day mass to be $\sim 10^6 M_\odot$ (Harris 1996, 2010 edition; Baumgardt & Hilker 2018; Ye et al. 2022), and that it lost about half of its mass in ~ 11 Gyr. For an initial cluster mass of $2 \times 10^6 M_\odot$, the number of MSPs estimated from Eq. 3 at 11 Gyr is about 9. We use a factor of about 2 for the 1σ upper limit and take

³ The catalog models assume a point-mass spherical Galactic potential, and do not take into account the tidal shocking effect of the Galactic disk, so they potentially underestimate the mass loss rate from this effect.

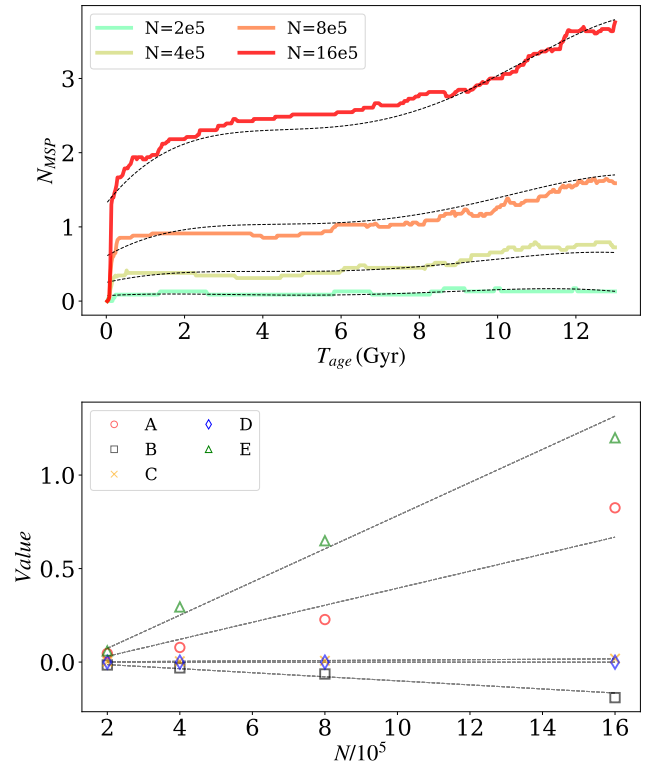


Figure 3. Top panel: The average number of MSPs for models with different initial number of stars, N , as a function of the cluster age. The solid curves represent the model averages, while the black dashed curves show the fits from Eq. 3. Bottom panel: the markers and the black dashed lines show the polynomial parameters and their fits from Eq. 3, respectively.

into account that $\sim 70\%$ of its MSPs may come from binary formation through giant star collisions with NSs and tidal capture interactions between a NS and a main-sequence star (Ye et al. 2022). The final estimated number of MSPs in 47 Tucanae at the present day is ~ 60 , consistent with the estimates from the previous targeted simulation of the cluster (Ye et al. 2022) and with the

observations (e.g., Heinke et al. 2005; Abdo et al. 2009). This example also demonstrates that our scaling relations can be used to estimate reasonably the number of MSPs in clusters with masses larger than the ones in the CMC catalog models.

3. APPLICATION TO THE GALACTIC-CENTER GAMMA-RAY EXCESS

In this Section, we adopt the semi-analytical method described in Gnedin et al. (2014) for building a Galactic potential, sampling an initial population of globular clusters, and inspiraling the clusters through dynamical friction into the Galactic Center (Section 3.1). We then use the masses of the inspiraled globular clusters to estimate the number of MSPs delivered to the Galactic Center and their gamma-ray emission (Section 3.2). This semi-analytical approach allows us to sample a large number of globular clusters without significant computational costs.

For the purpose of estimating the number of MSPs in the Galactic Center from inspiraling globular cluster, we also calculate the average MSPs for all models with initial $R_g = 2$ kpc (including dissolved models). Here, we only consider models with $R_g = 2$ kpc because they can most closely represent the inspiraling globular clusters affected strongly by the Galactic potential. The polynomial fits as a function of the cluster age and the initial cluster mass are as follows

$$\begin{aligned}
 N_{MSP} &= A_{rg2} \times t + B_{rg2} \times t^2 + C_{rg2} \times t^3 + D_{rg2}, \\
 A_{rg2} &= 0.018 \times M_5 - 0.009, \\
 B_{rg2} &= -0.0030 \times M_5 + 0.0015, \\
 C_{rg2} &= 0.0002 \times M_5 - 0.0002, \\
 D_{rg2} &= 0.068 \times M_5 - 0.157.
 \end{aligned} \tag{4}$$

Figure 4 compares the fits to the model data. When compared to the fits using all models as in Figure 3, we find that there could be larger deviations, especially for initial $N = 8 \times 10^5$ in Figure 4 (top panel). This is probably due to the fact that the number of models is smaller (48 models with $R_g = 2$ kpc compared to 119 total non-dissolved models). Note that we include both not-yet-dissolved and non-dissolved models in this calculation.

3.1. Semi-analytical Methods

We briefly summarize the semi-analytical methods from Gnedin et al. (2014). We assume that the Galaxy is composed of stars whose distribution follows a spherical Sérsic mass density profile (e.g., Terzić & Graham 2005), and a dark matter halo with an Navarro–Frenk–White

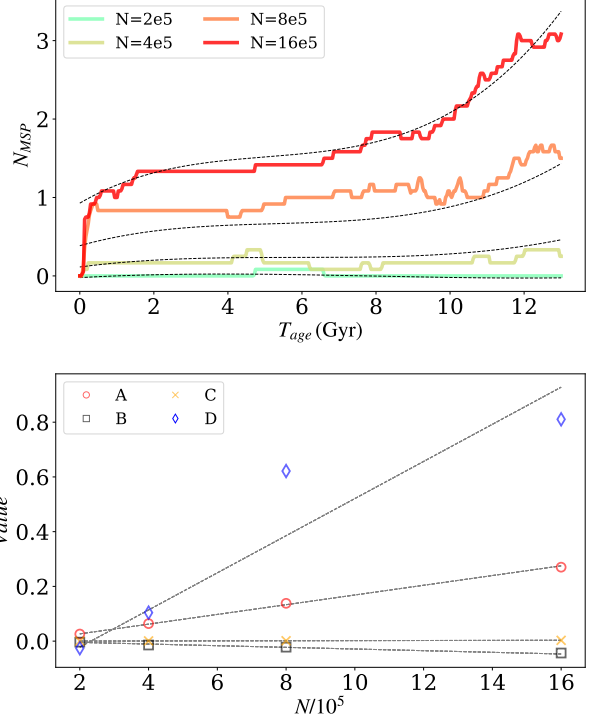


Figure 4. Similar to Figure 3, but only for models with a Galactocentric distance $R_g = 2$ kpc.

profile (Binney & Tremaine 2008). The Sérsic profile has a total mass $M_s = 5 \times 10^{10} M_\odot$, a concentration index $n_s = 2.2$, and an effective radius $R_s = 4$ kpc. The Navarro–Frenk–White profile has a total mass $M_h = 10^{12} M_\odot$, and a scale radius $R_h = 20$ kpc. In addition, we also include a central supermassive black hole with a mass $M_{SMBH} = 4 \times 10^6 M_\odot$.

To initialize a population of globular clusters, we assume that they follow the mass distributions of the stars in the Galaxy, and their total mass is a fixed fraction, 1.2%, of the field stars (Gnedin et al. 2014). We also assume that clusters are on circular orbits, and sample their initial semi-major axes in the Galaxy between 0.1 and 100 kpc. The individual masses of the globular clusters are drawn from a power-law distribution

$$\frac{dN_{GC}}{dM_{GC}} \propto M_{GC}^{-2}, \tag{5}$$

where N_{GC} is the number of globular clusters at a certain mass, and M_{GC} is the cluster mass, in the range $10^4 M_\odot$ – $10^7 M_\odot$. Finally, we adopt the average density at the half-mass radius

$$\rho_h = 10^3 \min \left\{ 10^2, \max \left[1, \left(\frac{M}{10^5 M_\odot} \right)^2 \right] \right\} \frac{M_\odot}{\text{pc}^3}. \tag{6}$$

Dynamical friction leads to the gradual inspiral of the globular clusters in the Galactic potential. We calculate the evolution of a cluster's distance to the Galactic center following (Binney & Tremaine 2008; Gnedin et al. 2014)

$$\frac{dr^2}{dt} = -\frac{r^2}{t_{df}}, \quad (7)$$

$$t_{df} \approx 0.23 \left(\frac{r}{\text{kpc}}\right)^2 \left(\frac{M_{GC}}{10^5 M_\odot}\right)^{-1} \left(\frac{v_c}{\text{km s}^{-1}}\right) \text{Gyr}, \quad (8)$$

where v_c is the circular orbital velocity of a globular cluster.

During inspiral, a globular cluster will lose mass from the stripping of stars by the Galactic tidal field, evaporation of stars through two-body relaxation, and stellar evolution. The timescale of mass loss from the stripping of stars by the Galactic tidal field can be estimated by (Gieles & Baumgardt 2008; Gnedin et al. 2014)

$$t_{tid} \approx 10 \left(\frac{M_{GC}}{2 \times 10^5 M_\odot}\right)^{2/3} P(r) \text{Gyr}, \quad (9)$$

where

$$P(r) = 41.4 \left(\frac{r}{\text{kpc}}\right) \left(\frac{v_c}{\text{km s}^{-1}}\right)^{-1}. \quad (10)$$

For isolated globular clusters, the evaporation time follows (Gnedin et al. 2014, and references therein)

$$t_{iso} = 17 \left(\frac{M_{GC}}{2 \times 10^5 M_\odot}\right) \text{Gyr}. \quad (11)$$

The mass loss rate of a globular cluster from these two effects is

$$\frac{dM_{GC}}{dt} = -\frac{M_{GC}}{\min(t_{iso}, t_{tid})}. \quad (12)$$

Typically, $t_{tid} < t_{iso}$ in the inner regions of the galaxy, which harbor the globular clusters that can potentially spiral into the Galactic Center. Finally, to incorporate mass loss from stellar evolution, we assume a broken-power-law IMF as in Kroupa (2001), with stellar masses between 0.08 and $150 M_\odot$. We model the initial-to-final mass relation following Merritt (2013, Eq. 7.22), and the turn-off mass at a given time is approximated using $m_{TO} \approx (t_{ms}/10 \text{Gyr})^{-2/5}$ (Hansen & Kawaler 1994). Note that the mass lost from the globular clusters is added to the field stellar mass at each time step.

We evolve our population of globular clusters for 11.5 Gyr assuming that all clusters formed from a burst of star formation at redshift $z = 3$ (Fragione et al. 2018). We classify globular clusters as disrupted when the cluster mass densities at their half-mass radii are

smaller than the surrounding Galactic field density, when $M_{GC} < 100 M_\odot$ (Harris 1996, 2010 edition; Baumgardt & Hilker 2018, also see Figure 5 below), or when its distance with respect to the Galactic Center is smaller than 1 pc.

3.2. Millisecond Pulsars and the Gamma-ray Excess in the Galactic Center

We sample about 8700 globular clusters with an initial total mass of about $5.4 \times 10^8 M_\odot$. We find that after 11.5 Gyr most of the globular clusters are disrupted, with only about 200 systems surviving to the present day, which is in nice agreement with the number of observed globular clusters in our Galaxy (Harris 1996, 2010 edition). Figure 5 compares the number density distribution and mass distribution of the survived sample globular clusters to the observations. The results from our simple semi-analytical method are consistent with most of the features in the observed population of Galactic globular clusters. In addition, since our semi-analytical method is based on the method from Gnedin et al. (2014, and references therein), where it was shown that the method reproduces broadly the properties (including masses and radii) of Milky Way globular clusters, the survived sample clusters should also have half-mass radii consistent with the observations.

We use Eq. 4 to estimate the number of MSPs delivered to the Galactic Center by inspiraling globular clusters⁴. In addition, a non-negligible number of MSPs are ejected from the globular clusters, where $\sim 90\%$ of them are ejected at $\lesssim 100 \text{Myr}$ ⁵. The number of ejected MSPs scales with the initial number of cluster stars N as $N_{\text{MSP, ej}} \approx \log_2(N/2 \times 10^5)$. Therefore, for simplicity, we add an ejected number of MSPs at the initial position of a globular cluster in the sample.

The number of MSPs brought by inspiraled globular clusters to the Galactic Center is shown in Figure 6. Note that the stellar mass contributed by our sample of inspiraled globular clusters are within the limits of the observed masses of the Milky Way nuclear star cluster, whose mass is equally contributed to from local star formation and inspiralled star clusters (Launhardt et al. 2002; Schödel et al. 2014a,b; top panel). We find that the number of MSPs within 2 kpc of the Galactic Center is about 400, with a 1σ upper limit (a factor of 2 in Eq. 3

⁴ We assume that all MSPs formed in a globular cluster that are not ejected stay close to the cluster center and do not get stripped during the gradual disruption of the outermost regions of their host globular clusters.

⁵ There are also ~ 15 NS-white dwarf and NS-main sequence star binaries ejected per cluster, some of which may become MSPs in the future. For simplicity we do not consider these systems.

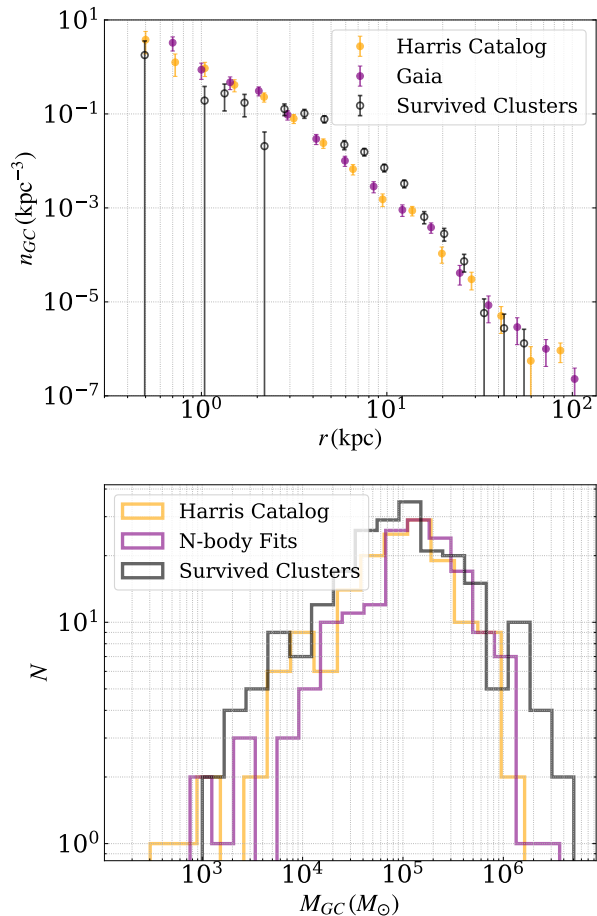


Figure 5. Top panel: Number density of globular clusters as a function of the Galactocentric distance in the Milky Way. The orange and purple dots show the observations from the Harris catalog (Harris 1996, 2010 edition) and the Gaia EDR3 (Baumgardt & Vasiliev 2021), respectively. The black dots show the survived globular clusters at 11.5 Gyr from our cluster samples. Bottom panel: Mass distribution of globular clusters in the Milky Way. The orange histogram is from the Harris catalog (Harris 1996, 2010 edition) assuming a mass-to-light ratio of 1.5. The purple histogram is from N -body fits to the observed cluster surface brightness profiles and velocity dispersion profiles (Baumgardt 2017; Baumgardt & Hilker 2018). The mass distribution of the survived sample clusters are shown in the black histogram.

as mentioned in Section 2.3) of about 500. While taking into account binary formation through giant star collisions with NSs and tidal capture of main-sequence stars by NSs, and assuming that 70% of MSPs are formed from these channels (Ye et al. 2022), the number of MSPs can be up to ~ 1000 (also taking into account the 1σ upper limit). However, it is important to point out that this is an optimistic upper limit since the 70% used is for a cluster like 47 Tucanae, which is one of the

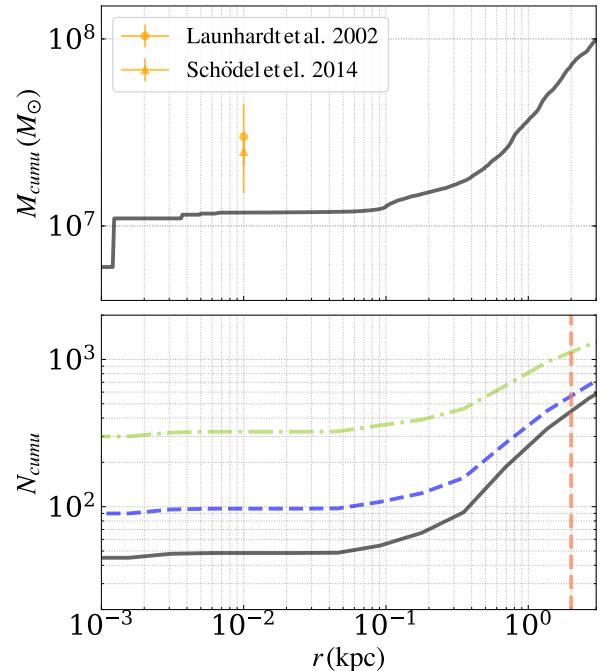


Figure 6. Top panel: Cumulative distribution of mass lost from the inspiraled globular clusters and mass from the remnants of the disrupted globular clusters. The orange markers show the observational constraints on the mass of the Milky Way nuclear star cluster (Launhardt et al. 2002; Schödel et al. 2014a,b). Bottom panel: Cumulative number of MSPs from the disrupted globular clusters, including MSPs that were ejected initially. The black curve is calculated from the averages of Eq. 4. The blue dashed curve is the 1σ upper limit from Eq. 3, while the green dot-dashed curve shows an extreme upper limit taking into account that 70% of the MSPs in a cluster can be formed from giant star collisions with NSs and tidal capture interactions (in addition to the 1σ upper limit), which were not considered in the catalog models. The vertical line marks 2 kpc.

most massive and densest globular clusters in the Milky Way, and is likely to have more dynamical interactions than typical globular clusters (Ye et al. 2022). Note that these numbers are consistent with the numbers predicted by gamma-ray luminosity functions (Dinsmore & Slatyer 2021).

In Figure 7, we show the gamma-ray surface brightness from the population of MSPs from inspiraled globular clusters, compared to the detected Galactic-Center gamma-ray excess (Hooper & Slatyer 2013; Calore et al. 2015; Daylan et al. 2016; Horiuchi et al. 2016; Di Mauro 2021). The gamma-ray surface brightness corresponds to the average number of MSPs estimated from disrupted clusters (the black curve in the bottom panel of Figure 6). The gamma-ray luminosity of each MSP

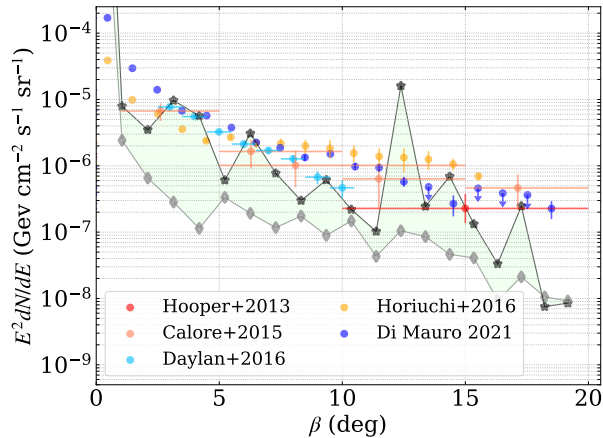


Figure 7. Gamma-ray surface brightness of MSPs from disrupted globular clusters and the gamma-ray excess detected around the Galactic Center as a function of the angular distance to the Galactic Center (Hooper & Slatyer 2013; Calore et al. 2015; Daylan et al. 2016; Horiuchi et al. 2016; Di Mauro 2021). The gamma-ray surface brightness of MSPs corresponds to the average number of MSPs shown by the black curve in Figure 6 (bottom panel). Black stars show the case where the MSP gamma-ray luminosities are calculated using Eq. 2, while gray diamonds assume that all MSPs have a gamma-ray luminosity of $4.8 \times 10^{33} \text{ erg s}^{-1}$.

is drawn randomly from a list of MSPs from all catalog models with initial $R_g = 2 \text{ kpc}$, depending on when the host cluster is disrupted or when the MSP is ejected. The large fluctuation (the black star at $\gtrsim 10^{-5} \text{ GeV cm}^{-2} \text{ s}^{-1} \text{ sr}^{-1}$) is resulted from random draws of MSPs with large gamma-ray luminosities. The average luminosity of these MSPs is $\sim 3 \times 10^{34} \text{ erg s}^{-1}$. For comparison, we also show in the figure the surface brightness profile when all MSPs have a gamma-ray luminosity of $4.8 \times 10^{33} \text{ erg s}^{-1}$ (gray diamonds; see also Eq. 2). We find that, for high gamma-ray luminosities $\sim 10^{34} \text{ erg s}^{-1}$ per MSP, MSPs from inspiraled globular clusters can potentially explain most of the detected excess. However, if MSPs have lower luminosities $\sim 10^{33} \text{ erg s}^{-1}$, they may only contribute to $\lesssim 10\%$ of the detected gamma-ray excess, consistent with the previous population synthesis study (Gonthier et al. 2018). For the extreme case where 70% of cluster MSPs come from the giant star collision and tidal capture channels, and including a factor of 2 for the 1σ upper limit, MSPs from disrupted globular clusters produce a gamma-ray surface brightness comparable to the observed gamma-ray excess if all MSPs have gamma-ray luminosity $\sim 10^{34} \text{ erg s}^{-1}$.

4. DISCUSSIONS AND CONCLUSIONS

To summarize, we have explored in this study how the initial conditions of dense star clusters affect the number of MSPs they produce using the CMC cluster catalog models (Kremer et al. 2020). We have presented scaling relations, which express the numbers of MSPs as a function of the cluster age for different initial cluster masses in Eq.s 3-4. Our scaling relations allow quick estimates of the number of MSPs in dense star clusters.

We have also demonstrated that our model MSPs can reproduce the gamma-ray luminosities observed from globular clusters. We have applied the scaling relation we have derived to estimate the number of MSPs delivered to the Galactic Center from inspiraled globular clusters. On average, about 400 MSPs are brought to the Galactic Center by globular clusters, with an optimistic upper limit ~ 1000 . These MSPs have an average gamma-ray luminosity $\sim 3 \times 10^{34} \text{ erg s}^{-1}$, and can potentially explain most of the detected gamma-ray excess from the Galactic Center.

There are a few uncertainties on the predicted number of MSPs from the catalog models. We have briefly mentioned one uncertainty in Section 2.3; that is, for massive and dense globular clusters, dynamical binary formation through NS-giant star collisions or tidal capture interactions may also contribute to a large portion of cluster MSPs ($\sim 70\%$ for massive and dense globular clusters similar to 47 Tucanae, see Ye et al. 2022). Furthermore, observations have shown that core-collapsed globular clusters contain more isolated MSPs, which could be formed from tidal disruption events between a NS and a main sequence star (Kremer et al. 2022). These effects combined together could contribute to a factor of a few in the number of MSPs formed in dense globular clusters, most of which are core-collapsed. However, only around 20% of the present-day globular clusters are core-collapsed (Harris 1996, 2010 edition), and if the fraction was similar for all clusters ever formed in the Milky Way, the boost from these dynamical interactions may not be very significant. In addition, we have only studied models with an initial binary fraction of 5%, but the rates of binary-mediated dynamical encounters could be significantly affected by different initial binary fractions. The catalog models also only adopt a standard Kroupa IMF (Kroupa 2001). However, studies have suggested that the IMF of globular clusters may not be universal (e.g., Marks et al. 2012; Hagi et al. 2017; Sollima & Baumgardt 2017; Cadelano et al. 2020; Hénault-Brunet et al. 2020), with different IMFs leading to different number of MSPs dynamically assembled in star clusters. For example, a top-heavy IMF (where there are more massive stars than the standard Kroupa IMF) will

produce more NSs and black holes, but more black holes on average lead to fewer dynamical interactions for NSs, therefore likely fewer MSPs (Ye et al. 2019). Similarly, a bottom-light IMF will produce more black holes per cluster mass, thus may also lead to few MSPs. Finally, the predicted number of MSPs in the Galactic Center is also limited by models that are only at the constant Galactocentric distance $R_g = 2$ kpc. In reality, orbits of globular clusters in a galaxy are not always circular (Vasiliev & Baumgardt 2021), and the galactic potential they are subjected to are time-dependant during inspiral. We leave the detailed exploration of the previous uncertainties to future work (Ye et al. in preparation).

1 We thank Fred Rasio, Kyle Kremer, Carl Rodriguez,
 2 and the anonymous referee for useful discussions and
 3 comments. This work was supported by NSF Grants
 4 AST-1716762, AST-2108624 at Northwestern Univer-
 5 sity, and by the Natural Sciences and Engineer-
 6 ing Research Council of Canada (NSERC) DIS-2022-
 7 568580. G.F. acknowledges support from NASA Grant
 8 80NSSC21K1722. This research was supported in part
 9 through the computational resources and staff contribu-
 10 tions provided for the Quest high performance comput-
 11 ing facility at Northwestern University, which is jointly
 12 supported by the Office of the Provost, the Office for Re-
 13 search, and Northwestern University Information Tech-
 14 nology.

Software: CMC (Joshi et al. 2000, 2001; Fregeau et al. 2003; Fregeau & Rasio 2007; Chatterjee et al. 2010; Umbreit et al. 2012; Chatterjee et al. 2013; Pattabiraman et al. 2013; Morscher et al. 2015; Rodriguez et al. 2016, 2021), Fewbody (Fregeau et al. 2004), COSMIC (Breivik et al. 2020), BSE (Hurley et al. 2002), SSE (Hurley et al. 2000)

APPENDIX

Similar to Figure 2, we show here the number of MSPs in the catalog models with all the combinations of different initial conditions.

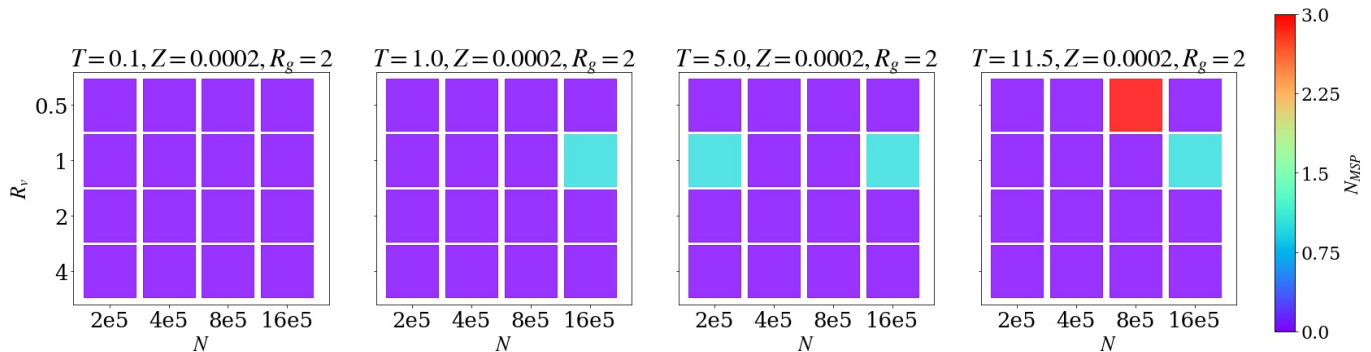


Figure 8. Same as Figure 2 but for models with a metallicity $Z = 0.0002$ and Galactocentric distance $R_g = 2$ kpc.

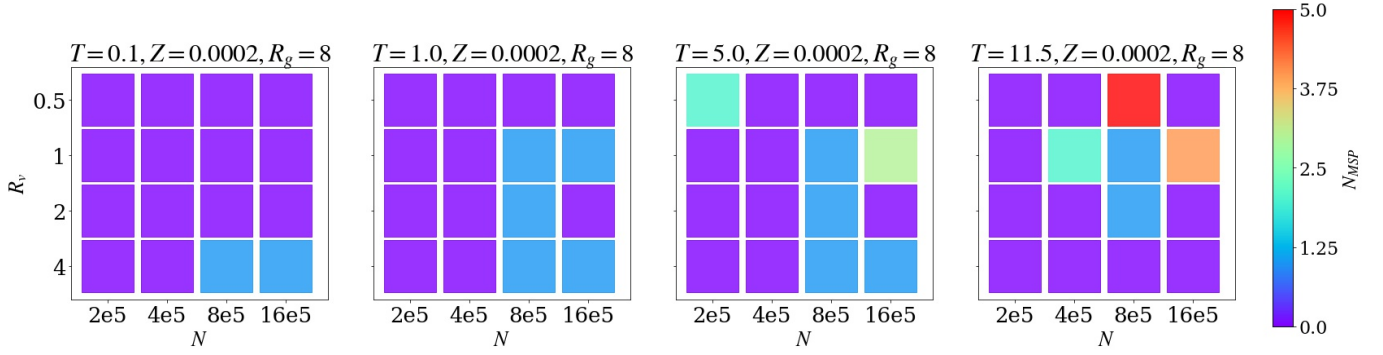


Figure 9. Same as Figure 2 but for models with a metallicity $Z = 0.0002$ and Galactocentric distance $R_g = 8$ kpc.

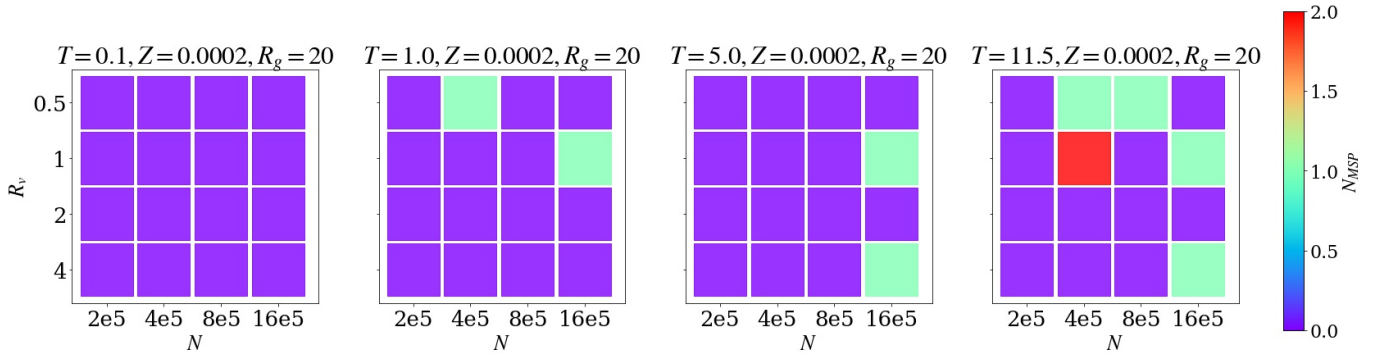


Figure 10. Same as Figure 2 but for models with a metallicity $Z = 0.0002$ and Galactocentric distance $R_g = 20$ kpc.

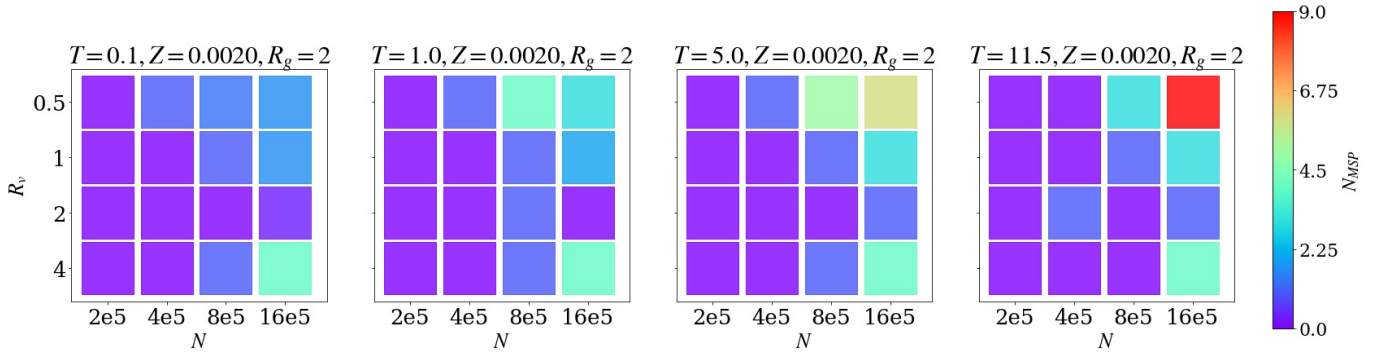


Figure 11. Same as Figure 2 but for models with a metallicity $Z = 0.002$ and Galactocentric distance $R_g = 2$ kpc.

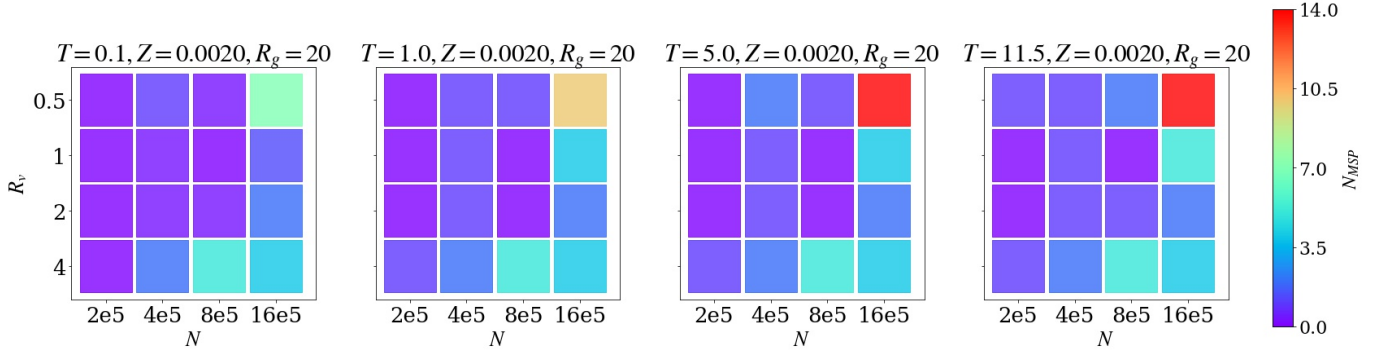


Figure 12. Same as Figure 2 but for models with a metallicity $Z = 0.002$ and Galactocentric distance $R_g = 20$ kpc.

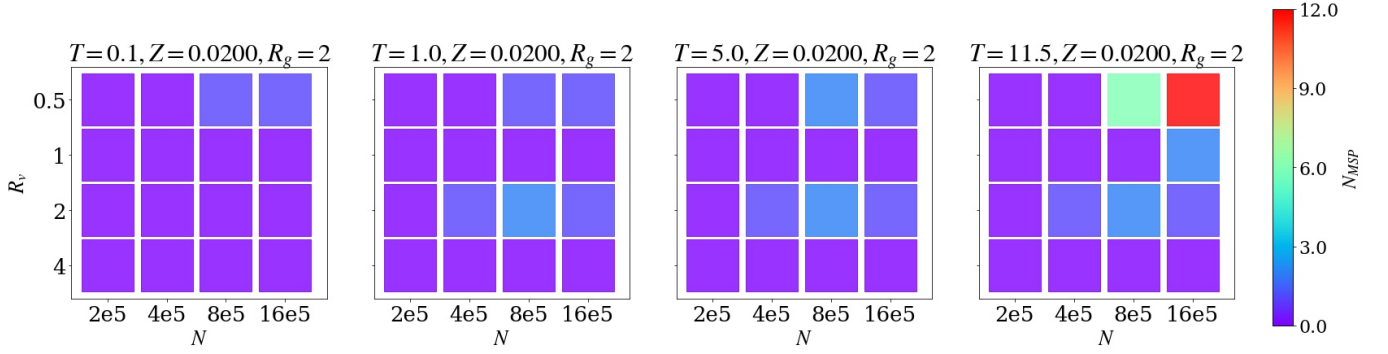


Figure 13. Same as Figure 2 but for models with a metallicity $Z = 0.02$ and Galactocentric distance $R_g = 2$ kpc.

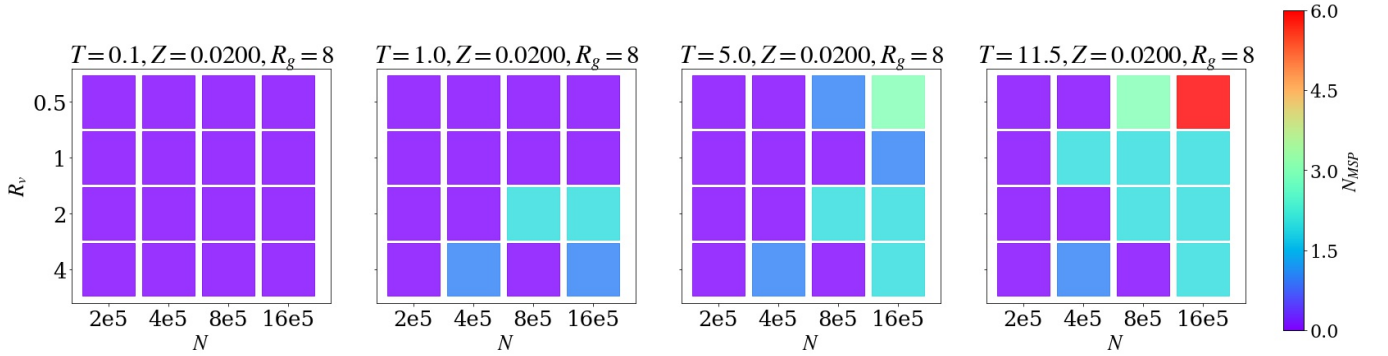


Figure 14. Same as Figure 2 but for models with a metallicity $Z = 0.02$ and Galactocentric distance $R_g = 8$ kpc.

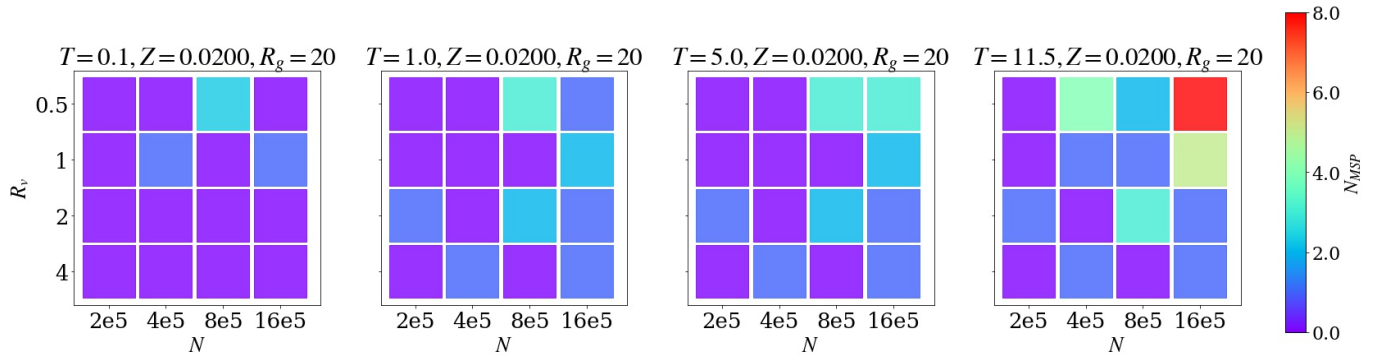


Figure 15. Same as Figure 2 but for models with a metallicity $Z = 0.02$ and Galactocentric distance $R_g = 20$ kpc.

REFERENCES

- Abazajian, K. N. 2011, JCAP, 2011, 010, doi: [10.1088/1475-7516/2011/03/010](https://doi.org/10.1088/1475-7516/2011/03/010)
- Abazajian, K. N., & Kaplinghat, M. 2012, PhRvD, 86, 083511, doi: [10.1103/PhysRevD.86.083511](https://doi.org/10.1103/PhysRevD.86.083511)
- Abbate, F., Mastrobuono-Battisti, A., Colpi, M., et al. 2018, MNRAS, 473, 927, doi: [10.1093/mnras/stx2364](https://doi.org/10.1093/mnras/stx2364)
- Abbott, B. P., Abbott, R., Abbott, T. D., et al. 2017, PhRvL, 119, 161101, doi: [10.1103/PhysRevLett.119.161101](https://doi.org/10.1103/PhysRevLett.119.161101)
- Abdo, A. A., Ackermann, M., Ajello, M., et al. 2009, Science, 325, 845, doi: [10.1126/science.1177023](https://doi.org/10.1126/science.1177023)
- . 2010, A&A, 524, A75, doi: [10.1051/0004-6361/201014458](https://doi.org/10.1051/0004-6361/201014458)
- Alpar, M. A., Cheng, A. F., Ruderman, M. A., & Shaham, J. 1982, Nature, 300, 728, doi: [10.1038/300728a0](https://doi.org/10.1038/300728a0)
- Bagchi, M., Lorimer, D. R., & Chennamangalam, J. 2011, MNRAS, 418, 477, doi: [10.1111/j.1365-2966.2011.19498.x](https://doi.org/10.1111/j.1365-2966.2011.19498.x)
- Baumgardt, H. 2017, MNRAS, 464, 2174, doi: [10.1093/mnras/stw2488](https://doi.org/10.1093/mnras/stw2488)
- Baumgardt, H., & Hilker, M. 2018, MNRAS, 478, 1520, doi: [10.1093/mnras/sty1057](https://doi.org/10.1093/mnras/sty1057)
- Baumgardt, H., & Vasiliev, E. 2021, MNRAS, 505, 5957, doi: [10.1093/mnras/stab1474](https://doi.org/10.1093/mnras/stab1474)
- Bhattacharya, D., & van den Heuvel, E. P. J. 1991, PhR, 203, 1, doi: [10.1016/0370-1573\(91\)90064-S](https://doi.org/10.1016/0370-1573(91)90064-S)
- Binney, J., & Tremaine, S. 2008, Galactic Dynamics: Second Edition
- Brandt, T. D., & Kocsis, B. 2015, ApJ, 812, 15, doi: [10.1088/0004-637X/812/1/15](https://doi.org/10.1088/0004-637X/812/1/15)
- Breivik, K., Coughlin, S., Zevin, M., et al. 2020, ApJ, 898, 71, doi: [10.3847/1538-4357/ab9d85](https://doi.org/10.3847/1538-4357/ab9d85)
- Cadelano, M., Dalessandro, E., Webb, J. J., et al. 2020, MNRAS, 499, 2390, doi: [10.1093/mnras/staa2759](https://doi.org/10.1093/mnras/staa2759)
- Calore, F., Cholis, I., & Weniger, C. 2015, JCAP, 2015, 038, doi: [10.1088/1475-7516/2015/03/038](https://doi.org/10.1088/1475-7516/2015/03/038)
- Chatterjee, S., Fregeau, J. M., Umbreit, S., & Rasio, F. A. 2010, ApJ, 719, 915, <http://dx.doi.org/10.1088/0004-637X/719/1/915>
- Chatterjee, S., Umbreit, S., Fregeau, J. M., & Rasio, F. A. 2013, MNRAS, 429, 2881, <http://dx.doi.org/10.1093/mnras/sts464>
- Cholis, I., Hooper, D., & Linden, T. 2015, JCAP, 2015, 043, doi: [10.1088/1475-7516/2015/06/043](https://doi.org/10.1088/1475-7516/2015/06/043)
- Clark, G. W. 1975, ApJL, 199, L143, doi: [10.1086/181869](https://doi.org/10.1086/181869)
- Daylan, T., Finkbeiner, D. P., Hooper, D., et al. 2016, Physics of the Dark Universe, 12, 1, doi: [10.1016/j.dark.2015.12.005](https://doi.org/10.1016/j.dark.2015.12.005)
- Di Mauro, M. 2021, PhRvD, 103, 063029, doi: [10.1103/PhysRevD.103.063029](https://doi.org/10.1103/PhysRevD.103.063029)
- Dinsmore, J. T., & Slatyer, T. R. 2021, arXiv e-prints, arXiv:2112.09699, <https://arxiv.org/abs/2112.09699>
- Dotter, A., Sarajedini, A., & Anderson, J. 2011, ApJ, 738, 74, doi: [10.1088/0004-637X/738/1/74](https://doi.org/10.1088/0004-637X/738/1/74)
- Dotter, A., Sarajedini, A., Anderson, J., et al. 2010, ApJ, 708, 698, doi: [10.1088/0004-637X/708/1/698](https://doi.org/10.1088/0004-637X/708/1/698)
- Duquennoy, A., & Mayor, M. 1991, A&A, 500, 337
- Forbes, D. A., & Bridges, T. 2010, MNRAS, 404, 1203, doi: [10.1111/j.1365-2966.2010.16373.x](https://doi.org/10.1111/j.1365-2966.2010.16373.x)
- Fragione, G., Antonini, F., & Gnedin, O. Y. 2018, MNRAS, 475, 5313, doi: [10.1093/mnras/sty183](https://doi.org/10.1093/mnras/sty183)
- Fregeau, J. M., Cheung, P., Portegies Zwart, S., & Rasio, F. 2004, MNRAS, 352, 1
- Fregeau, J. M., Gurkan, M. A., Joshi, K. J., & Rasio, F. A. 2003, ApJ, 593, 772, <http://dx.doi.org/10.1086/376593>
- Fregeau, J. M., & Rasio, F. A. 2007, ApJ, 658, 1047
- Fruchter, A. S., & Goss, W. M. 1990, ApJL, 365, L63, doi: [10.1086/185889](https://doi.org/10.1086/185889)
- Gautam, A., Crocker, R. M., Ferrario, L., et al. 2022, Nature Astronomy, doi: [10.1038/s41550-022-01658-3](https://doi.org/10.1038/s41550-022-01658-3)
- Gieles, M., & Baumgardt, H. 2008, MNRAS, 389, L28, doi: [10.1111/j.1745-3933.2008.00515.x](https://doi.org/10.1111/j.1745-3933.2008.00515.x)

- Gnedin, O. Y., Ostriker, J. P., & Tremaine, S. 2014, *ApJ*, 785, 71, doi: [10.1088/0004-637X/785/1/71](https://doi.org/10.1088/0004-637X/785/1/71)
- Gonthier, P. L., Harding, A. K., Ferrara, E. C., et al. 2018, *ApJ*, 863, 199, doi: [10.3847/1538-4357/aad08d](https://doi.org/10.3847/1538-4357/aad08d)
- Goodenough, L., & Hooper, D. 2009, arXiv e-prints, arXiv:0910.2998. <https://arxiv.org/abs/0910.2998>
- Haggard, D., Heinke, C., Hooper, D., & Linden, T. 2017, *JCAP*, 2017, 056, doi: [10.1088/1475-7516/2017/05/056](https://doi.org/10.1088/1475-7516/2017/05/056)
- Haghi, H., Khalaj, P., Hasani Zonoozi, A., & Kroupa, P. 2017, *ApJ*, 839, 60, doi: [10.3847/1538-4357/aa6719](https://doi.org/10.3847/1538-4357/aa6719)
- Hansen, C. J., & Kawaler, S. D. 1994, *Stellar Interiors. Physical Principles, Structure, and Evolution.*, doi: [10.1007/978-1-4419-9110-2](https://doi.org/10.1007/978-1-4419-9110-2)
- Harris, W. E. 1996, *AJ*, 112, 1487, doi: [10.1086/118116](https://doi.org/10.1086/118116)
- Heggie, D. C. 1975, *MNRAS*, 173, 729, doi: [10.1093/mnras/173.3.729](https://doi.org/10.1093/mnras/173.3.729)
- Heinke, C. O., Grindlay, J. E., Edmonds, P. D., et al. 2005, *ApJ*, 625, 796, doi: [10.1086/429899](https://doi.org/10.1086/429899)
- Hénault-Brunet, V., Gieles, M., Strader, J., et al. 2020, *MNRAS*, 491, 113, doi: [10.1093/mnras/stz2995](https://doi.org/10.1093/mnras/stz2995)
- Hénon, M. 1971a, in *International Astronomical Union Colloquium, Vol. 10*, Cambridge University Press, 151–167
- Hénon, M. 1971b, *Ap&SS*, 13, 284
- Hewish, A., Bell, S. J., Pilkington, J. D. H., Scott, P. F., & Collins, R. A. 1968, *Nature*, 217, 709, doi: [10.1038/217709a0](https://doi.org/10.1038/217709a0)
- Hobbs, G., Lorimer, D. R., Lyne, A. G., & Kramer, M. 2005, *MNRAS*, 360, 974, doi: [10.1111/j.1365-2966.2005.09087.x](https://doi.org/10.1111/j.1365-2966.2005.09087.x)
- Hooper, D., & Goodenough, L. 2011, *Physics Letters B*, 697, 412, doi: [10.1016/j.physletb.2011.02.029](https://doi.org/10.1016/j.physletb.2011.02.029)
- Hooper, D., & Linden, T. 2011, *PhRvD*, 84, 123005, doi: [10.1103/PhysRevD.84.123005](https://doi.org/10.1103/PhysRevD.84.123005)
- . 2016, *JCAP*, 2016, 018, doi: [10.1088/1475-7516/2016/08/018](https://doi.org/10.1088/1475-7516/2016/08/018)
- Hooper, D., & Mohlabeng, G. 2016, *JCAP*, 2016, 049, doi: [10.1088/1475-7516/2016/03/049](https://doi.org/10.1088/1475-7516/2016/03/049)
- Hooper, D., & Slatyer, T. R. 2013, *Physics of the Dark Universe*, 2, 118, doi: [10.1016/j.dark.2013.06.003](https://doi.org/10.1016/j.dark.2013.06.003)
- Horiuchi, S., Kaplinghat, M., & Kwa, A. 2016, *JCAP*, 2016, 053, doi: [10.1088/1475-7516/2016/11/053](https://doi.org/10.1088/1475-7516/2016/11/053)
- Hui, C. Y., Cheng, K. S., & Taam, R. E. 2010, *ApJ*, 714, 1149, doi: [10.1088/0004-637X/714/2/1149](https://doi.org/10.1088/0004-637X/714/2/1149)
- Hurley, J. R., Pols, O. R., & Tout, C. A. 2000, *MNRAS*, 315, 543
- Hurley, J. R., Tout, C. A., & Pols, O. R. 2002, *MNRAS*, 329, 897
- Ivanova, N., Heinke, C. O., Rasio, F. A., Belczynski, K., & Fregeau, J. M. 2008, *MNRAS*, 386, 553, doi: [10.1111/j.1365-2966.2008.13064.x](https://doi.org/10.1111/j.1365-2966.2008.13064.x)
- Joshi, K. J., Nave, C. P., & Rasio, F. A. 2001, *ApJ*, 550, 691. <http://dx.doi.org/10.1086/319771>
- Joshi, K. J., Rasio, F. A., & Portegies Zwart, S. 2000, *ApJ*, 540, 969. <http://dx.doi.org/10.1086/309350>
- Kaspi, V. M. 2010, *Proceedings of the National Academy of Science*, 107, 7147, doi: [10.1073/pnas.1000812107](https://doi.org/10.1073/pnas.1000812107)
- Katz, J. I. 1975, *Nature*, 253, 698, doi: [10.1038/253698a0](https://doi.org/10.1038/253698a0)
- Kiel, P. D., Hurley, J. R., Bailes, M., & Murray, J. R. 2008, *MNRAS*, 388, 393, doi: [10.1111/j.1365-2966.2008.13402.x](https://doi.org/10.1111/j.1365-2966.2008.13402.x)
- King, I. R. 1966, *AJ*, 71, 64, doi: [10.1086/109857](https://doi.org/10.1086/109857)
- Kremer, K., Ye, C. S., Kiroğlu, F., et al. 2022, arXiv e-prints, arXiv:2204.07169. <https://arxiv.org/abs/2204.07169>
- Kremer, K., Ye, C. S., Rui, N. Z., et al. 2020, *ApJS*, 247, 48, doi: [10.3847/1538-4365/ab7919](https://doi.org/10.3847/1538-4365/ab7919)
- Kroupa, P. 2001, *MNRAS*, 322, 231
- Kruijssen, J. M. D., Pfeffer, J. L., Reina-Campos, M., Crain, R. A., & Bastian, N. 2019, *MNRAS*, 486, 3180, doi: [10.1093/mnras/sty1609](https://doi.org/10.1093/mnras/sty1609)
- Kulkarni, S. R., Narayan, R., & Romani, R. W. 1990, *ApJ*, 356, 174, doi: [10.1086/168828](https://doi.org/10.1086/168828)
- Launhardt, R., Zylka, R., & Mezger, P. G. 2002, *A&A*, 384, 112, doi: [10.1051/0004-6361:20020017](https://doi.org/10.1051/0004-6361:20020017)
- Lorimer, D. R. 2008, *Living Reviews in Relativity*, 11, 8, doi: [10.12942/lrr-2008-8](https://doi.org/10.12942/lrr-2008-8)
- Marks, M., Kroupa, P., Dabringhausen, J., & Pawlowski, M. S. 2012, *MNRAS*, 422, 2246, doi: [10.1111/j.1365-2966.2012.20767.x](https://doi.org/10.1111/j.1365-2966.2012.20767.x)
- Merritt, D. 2013, *Dynamics and Evolution of Galactic Nuclei*
- Morscher, M., Pattabiraman, B., Rodriguez, C., Rasio, F. A., & Umbreit, S. 2015, *ApJ*, 800, 9, doi: [10.1088/0004-637X/800/1/9](https://doi.org/10.1088/0004-637X/800/1/9)
- Murgia, S. 2020, *Annual Review of Nuclear and Particle Science*, 70, 455, doi: [10.1146/annurev-nucl-101916-123029](https://doi.org/10.1146/annurev-nucl-101916-123029)
- Naiman, J. P., Soares-Furtado, M., & Ramirez-Ruiz, E. 2020, *MNRAS*, 491, 4602, doi: [10.1093/mnras/stz3353](https://doi.org/10.1093/mnras/stz3353)
- Pan, Z., Qian, L., Ma, X., et al. 2021, *ApJL*, 915, L28, doi: [10.3847/2041-8213/ac0bbd](https://doi.org/10.3847/2041-8213/ac0bbd)
- Pattabiraman, B., Umbreit, S., Liao, W.-k., et al. 2013, *ApJS*, 204, 15. <http://dx.doi.org/10.1088/0067-0049/204/2/15>
- Petroff, E., Hessels, J. W. T., & Lorimer, D. R. 2022, *A&A Rv*, 30, 2, doi: [10.1007/s00159-022-00139-w](https://doi.org/10.1007/s00159-022-00139-w)

- Ransom, S. M. 2008, in *Dynamical Evolution of Dense Stellar Systems*, ed. E. Vesperini, M. Giersz, & A. Sills, Vol. 246, 291–300, doi: [10.1017/S1743921308015810](https://doi.org/10.1017/S1743921308015810)
- Ridolfi, A., Gautam, T., Freire, P. C. C., et al. 2021, *MNRAS*, 504, 1407, doi: [10.1093/mnras/stab790](https://doi.org/10.1093/mnras/stab790)
- Rodriguez, C. L., Morscher, M., Wang, L., et al. 2016, *MNRAS*, 463, 2109, doi: [10.1093/mnras/stw2121](https://doi.org/10.1093/mnras/stw2121)
- Rodriguez, C. L., Weatherford, N. C., Coughlin, S. C., et al. 2021, arXiv e-prints, arXiv:2106.02643. <https://arxiv.org/abs/2106.02643>
- Schödel, R., Feldmeier, A., Kunneriath, D., et al. 2014a, *A&A*, 566, A47, doi: [10.1051/0004-6361/201423481](https://doi.org/10.1051/0004-6361/201423481)
- Schödel, R., Feldmeier, A., Neumayer, N., Meyer, L., & Yelda, S. 2014b, *Classical and Quantum Gravity*, 31, 244007, doi: [10.1088/0264-9381/31/24/244007](https://doi.org/10.1088/0264-9381/31/24/244007)
- Sigurdsson, S., & Phinney, E. S. 1995, *ApJS*, 99, 609, doi: [10.1086/192199](https://doi.org/10.1086/192199)
- Sollima, A., & Baumgardt, H. 2017, *MNRAS*, 471, 3668, doi: [10.1093/mnras/stx1856](https://doi.org/10.1093/mnras/stx1856)
- Terzić, B., & Graham, A. W. 2005, *MNRAS*, 362, 197, doi: [10.1111/j.1365-2966.2005.09269.x](https://doi.org/10.1111/j.1365-2966.2005.09269.x)
- Turk, P. J., & Lorimer, D. R. 2013, *MNRAS*, 436, 3720, doi: [10.1093/mnras/stt1850](https://doi.org/10.1093/mnras/stt1850)
- Umbreit, S., Fregeau, J. M., Chatterjee, S., & Rasio, F. A. 2012, *ApJ*, 750, 31. <http://dx.doi.org/10.1088/0004-637X/750/1/31>
- VandenBerg, D. A., Brogaard, K., Leaman, R., & Casagrande, L. 2013, *ApJ*, 775, 134, doi: [10.1088/0004-637X/775/2/134](https://doi.org/10.1088/0004-637X/775/2/134)
- Vasiliev, E., & Baumgardt, H. 2021, *MNRAS*, 505, 5978, doi: [10.1093/mnras/stab1475](https://doi.org/10.1093/mnras/stab1475)
- Wijers, R. A. M. J., & van Paradijs, J. 1991, *A&A*, 241, L37
- Ye, C. S., Kremer, K., Chatterjee, S., Rodriguez, C. L., & Rasio, F. A. 2019, *ApJ*, 877, 122, doi: [10.3847/1538-4357/ab1b21](https://doi.org/10.3847/1538-4357/ab1b21)
- Ye, C. S., Kremer, K., Ransom, S. M., & Rasio, F. A. in preparation
- Ye, C. S., Kremer, K., Rodriguez, C. L., et al. 2022, *ApJ*, 931, 84, doi: [10.3847/1538-4357/ac5b0b](https://doi.org/10.3847/1538-4357/ac5b0b)